AXIALLY LOADED SEMI-ELLIPTICAL HOLLOW SECTION COLUMNS

M. M. FAWZY[1]

ABSTRACT

Complementary to studies of the cross-sectional behaviour of semi-elliptical hollow columns, investigations are conducted to study their behaviour about their minor axis. Section local and global non-dimensional slenderness values along with aspect ratio are carefully studied to cover a wide range. Two modes of failure of semi-elliptical hollow columns are observed: global and local. Increasing local slenderness can lead to a decrease in the section capacity by up to 100%. The increase in the aspect ratio decreases results by up to 95% in global non-dimensional slenderness of >1.23. Available equations in the Eurocode and Egyptian code for doubly symmetric compression members are used in the comparison with the analytical solution because there are no design equations specially for these columns. Good agreement is observed in the Eurocode for aspect ratios of 1 and 1.5. Egyptian code exhibits a <12% variation in results for these columns with global non-dimensional slenderness of <1.23, but it is found to be conservative for other columns. When the aspect ratio is 2, both codes become inaccurate, especially with compact sections where global non-dimensional slenderness is <1.23. Accordingly, design equations are prepared based on the analytical results where good agreement of results is obtained.

KEYWORDS: Semi-elliptical, Hollow, Columns, Non-dimensional slenderness, Local slenderness.

1. INTRODUCTION

A semi-elliptical hollow section (SEHS) is half of an ellipse connected to a flat part. Compared to circular hollow cross sections with the same area, these cross sections are usually more economical to produce. This is attributed to the fact that the effective radius of gyration of the minor axis is relatively smaller than that of the major axis. There are no design equations specifically addressing these columns. Accordingly, they are not widely used, although the presence of the flat part facilitates connections

---

[1] Assistant Professor, Department of Civil Engineering, Higher Institute of Engineering, El-Shorouk Academy, Cairo, Egypt, m.fawzy@sha.edu.eg

between columns and beam columns and they are also preferred by architects. No experimental testing has been conducted on SEHS cross sections in past research [1, 6]. However, research on the structural behaviour of elliptical hollow section columns has included testing, numerical modelling, and the development of design rules for cross sections in compression and bending, concrete-filled columns, beams, and beam columns [2–8]. The only analytical past research conducted related to SEHS columns focused on a series of geometric and material nonlinear finite element analyses. The studied parameters included different lengths and cross sections. Based on the results obtained from numerical methods, a comparison was conducted with the Eurocode (EURO) [9], but some numerical results exceeded the code standard by up to 65% [1, 8]. Accordingly, an obvious lack of data on the behaviour of SEHS columns indicates the need for further research on this topic. Therefore, an analytical investigation on the behaviour of SEHS members is conducted. Finally, the validity of different design codes is examined by comparing their results to numerical ones.

2. FINITE ELEMENT MODEL AND VERIFICATION

2.1 General Aspects

An ANSYS model was prepared with different dimensions. Shell element SHELL93 was used particularly for curved shells. Each node can make three translations and three rotations. The symbols used in the study are shown in Fig. 1: B is the width of the flat part (and was taken as 200, 300, and 400 mm), H is the width of the curved part (and was set to 200 mm), and t is the thickness of the column. The model consisted of elements with a reasonable aspect ratio of ~1, as shown in Fig. 2. The global imperfection used to study the behaviour of the SEHS column was $L/1000$ about the minor axis. Residual stresses were not explicitly incorporated into the numerical models according to past research [1] because they have been found to be very low in hot finished elliptical tubes. Incremental loading using a Newton–Raphson solver available in the ANSYS finite element program was used.
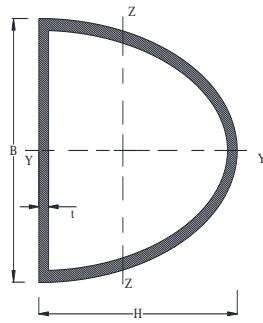
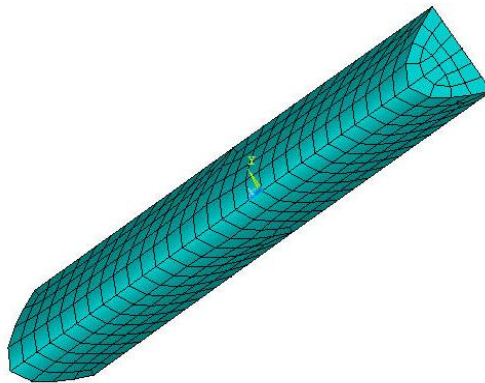Fig. 1. Cross-sectional dimensions.

Fig. 2. Finite element model meshing.

The effect of cross-sectional local slenderness (B/t), aspect ratio (B/H), and global non-dimensional slenderness (λ) was calculated by using

$$\lambda = \frac{KL}{\pi r} \sqrt{\frac{F_y}{E}} \tag{1}$$

where K is the buckling length factor, L is the unsupported length, r is the radius of gyration, F_y is the yield stress, and E is the modulus of elasticity of steel. The specimen lengths were carefully chosen to provide a spectrum of member slenderness. The studied λ range was from 0.29 to 3.38. B/t ratios were set as 25, 33 and 50, and B/H ratios were 1, 1.5, and 2. $B/t = 25$ represents compact sections, $B/t = 33$ represents noncompact sections, and $B/t = 50$ represent slender sections according to the Egyptian code (ECP) [10] and EURO [9]. The classification of section slenderness is listed in Table 1.

Table 1. SEHS classification according to ECP and EURO.

Code	B/t limits (code equation) for the flat part		
	Compact	Noncompact	Slender
ECP [10]	$B/t \leq 58/\sqrt{F_y}$	$B/t \leq 64/\sqrt{F_y}$	$B/t > 64/\sqrt{F_y}$
EURO	Class 1	Class 2	Class 3 Class 4
	$B/t \leq 33\varepsilon$	$B/t \leq 38\varepsilon$	$B/t \leq 42\varepsilon$ $B/t > 42\varepsilon$

2.2 Boundary Conditions and Load Application

A concentrated load was applied at the upper end plate in the centroid. Both end supports were prevented from translating in any directions except for the loaded end. Rotation about the longitudinal axis was prevented as well.

2.3 Finite Element Model Application

The finite element model was verified by comparing it with another research study about the buckling behaviour of SEHS columns under compression [8]. An ANSYS model was prepared with different dimensions as given in Table 2. In the former study, different columns, materials, and section lengths were investigated. The aspect ratio of the finite element model used was ~ 1. The authors of [8] also compared the ultimate loads of their finite element model with those of EURO. Table 1 lists a comparison between the ultimate loads of finite element models prepared here (FEM) and values from the previous research [8]. Good agreement in results can be observed. Consequently, this model can be used in the parametric study.

Table 2. Comparison between the present ultimate loads of finite element models prepared in this study and those from previous research [8].

Section ($H{\times}B{\times}t$) (mm)	Yield strength (MPa)	Length (mm)	EURO (kN)	Piers (kN)	FEM (kN)	FEM/EURO	FEM/Piers
203×223×8	355	1500	1917	1965.1	1884	0.98	0.96
		2500	1908.7	1966.2	1966	1.03	1.00
203×223×5	355	1500	1026.1	1179.7	1022	1.00	0.87
		2500	1019.6	1166.8	1145	1.12	0.98
	750	2500	1852	2237.2	1858	1.00	0.83
					Mean	1.03	0.93
					Standard deviation	0.06	0.07

3. RESULTS AND DISCUSSION

Normalised compressive strength, which is the ratio between the ultimate load of the FEM used in the parametric study and the yield load (FEM/P_Y), was used to compare

the results. P_Y is obtained by multiplying the yield stress and the semi-elliptical cross-sectional area. The effective area was used in the calculations of slender sections [3]. Two modes of SEHS failure were observed, i.e., global and local. Global buckling includes the great majority of long columns with the thickest SEHS walls, as shown in Fig. 3, where, in compact sections, local buckling is restrained until yielding of the section occurs. Meanwhile, local buckling, as shown in Fig. 4, occurs in the plate zone for slender sections with $\lambda \geq 1.23$. When $\lambda < 1.23$, slender sections buckle by local buckling, which occurs just before yielding.
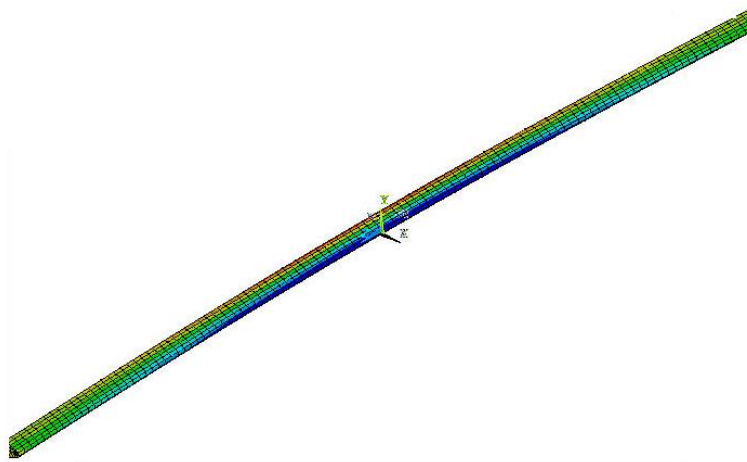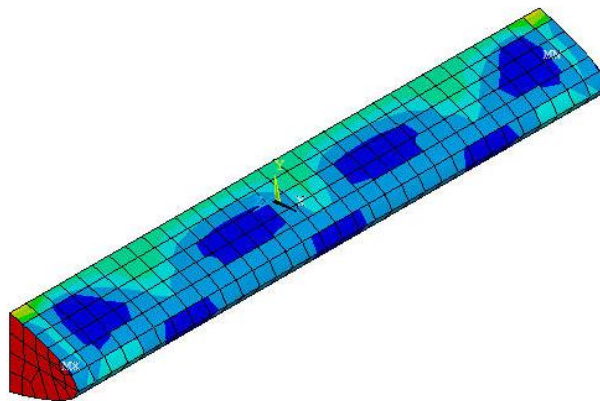
Fig. 3. Global buckling.

Fig. 4. Local buckling.

3.1   Behaviour of SESH Columns

3.1.1   Effect of cross-sectional local slenderness

For columns with $B/H = 1.0$ as shown in Fig. 5, changing the ratio of B/t from 25 to 50 causes an increase in the ultimate load to yield ratio (FEM/P_Y) by up to 28% for λ < 1.23, whereas a decrease by up to 68% is noticed for higher λ. Changing B/t from 33 to 50 causes an increase in FEM/P_Y by up to 34% for λ < 1.23. However, higher λ exhibits a decrease in FEM/P_Y by up to 92%. These results are attributed to the semi-elliptical part, which postpones failure in the postcritical strength of the straight slender sections only for lower λ.

When B/t ratio is changed from 25 or 33 to 50 for columns where $B/H = 1.5$, as shown in Fig. 6, FEM/P_Y decreases along with an increase in λ by >100%. Similarly, FEM/P_Y of sections with $B/H = 2$, as shown in Fig. 7, decrease by 93% because of the shifting of the B/t ratio from 33 to 50. When increasing the B/t ratio of the semi-elliptical part, prebuckling occurs, accompanied with postbuckling behaviour of the flat part, as shown in Fig. 8.
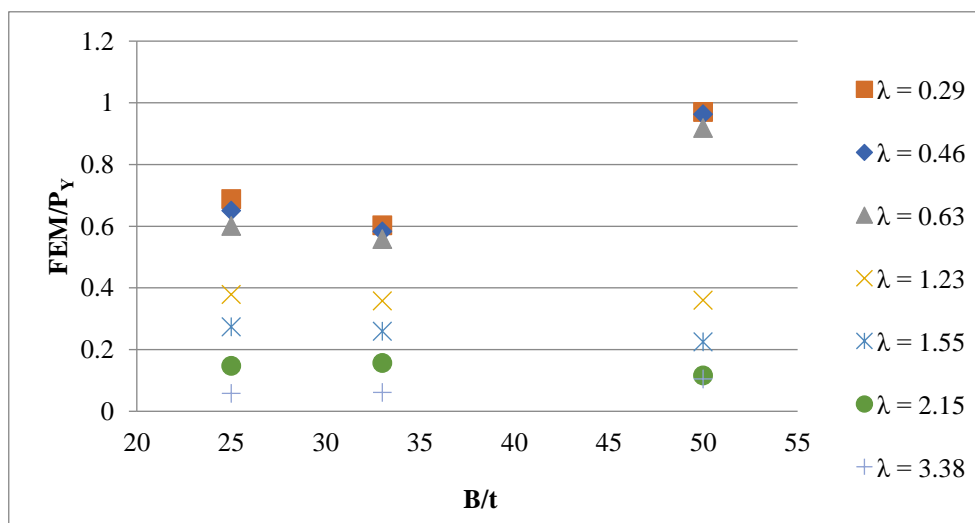

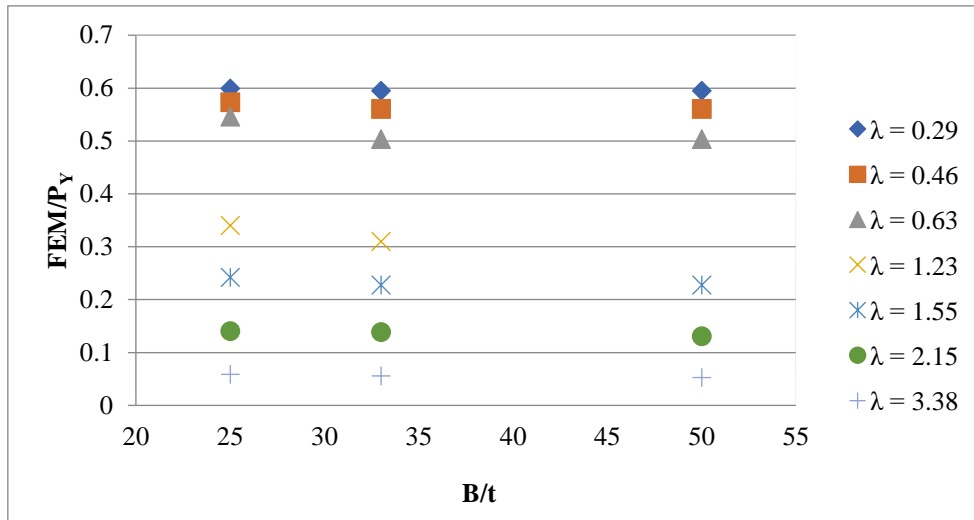Fig. 5. Relationship between B/t and FEM/P_Y for columns with $B/H = 1$.

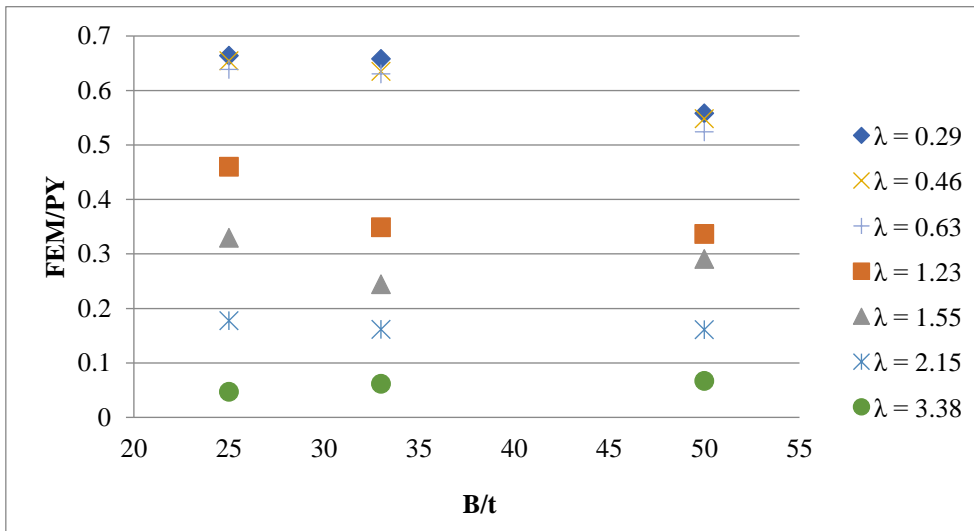Fig. 6. Relationship between B/t and FEM/P_Y for columns with $B/H = 1.5$.

Fig. 7. Relationship between B/t and FEM/P_Y for columns with $B/H = 2$.

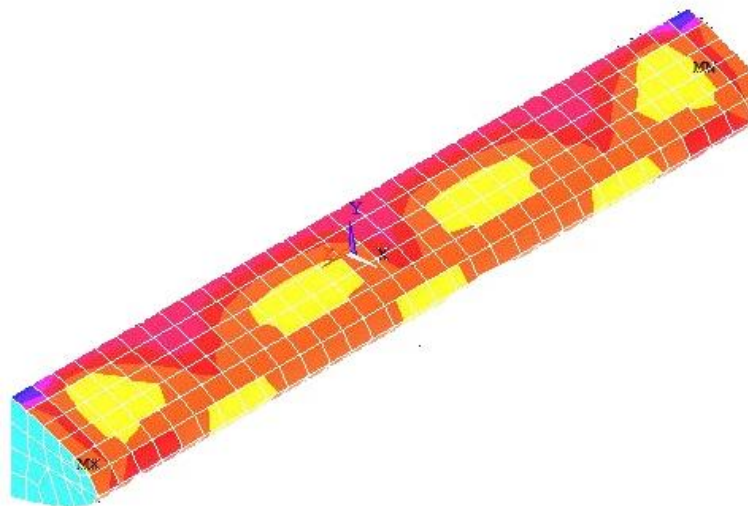

Fig. 8. Pre-buckling of a semi-elliptical section.

3.1.2 Effect of aspect ratio

According to Figs. 9-12, changing the aspect ratio (B/H) from 1 to 1.5 in columns with $B/t = 25$ and 33 decreases FEM/P_Y by up to 45% for $\lambda < 1.23$ and by up to 94% for higher values. This ratio in columns with $B/t = 50$ exhibits a decrease in FEM/P_Y by 49% for $\lambda < 1.23$ and by up to 94% for higher values. Similarly, changing the B/H ratio from 1 to 2 in columns with $B/t = 25$ and 33 decreases FEM/P_Y by 36% for $\lambda < 1.23$ and by 95% for higher values. Meanwhile, for columns with $B/t = 50$, FEM/P_Y decreases by 47% and by up to 93% for higher values. That decrease results from the contribution of the flat part to the strength and the fact that it has a much lower buckling stress than the SEHS part.
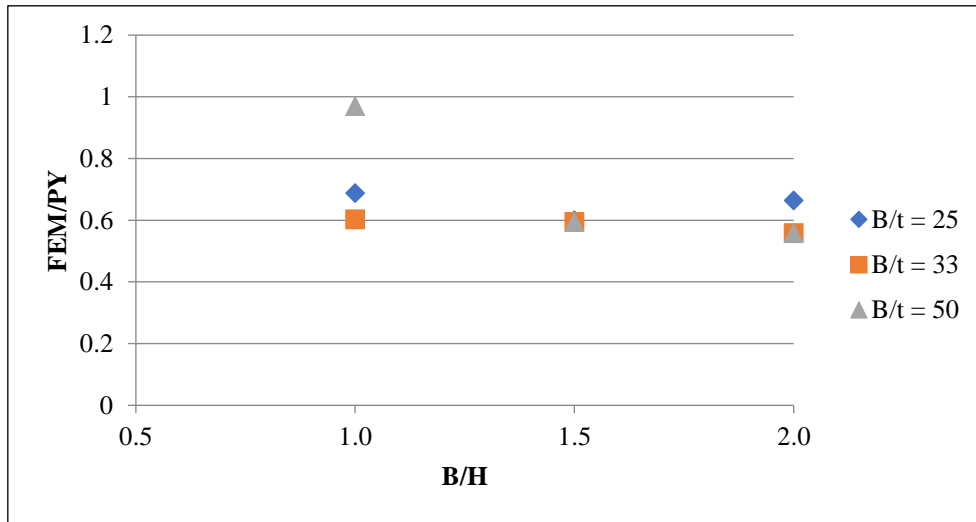

Fig. 9. Relationship between B/H and FEM/P_Y for columns with different B/t values and a slenderness ratio (λ) of 0.29.

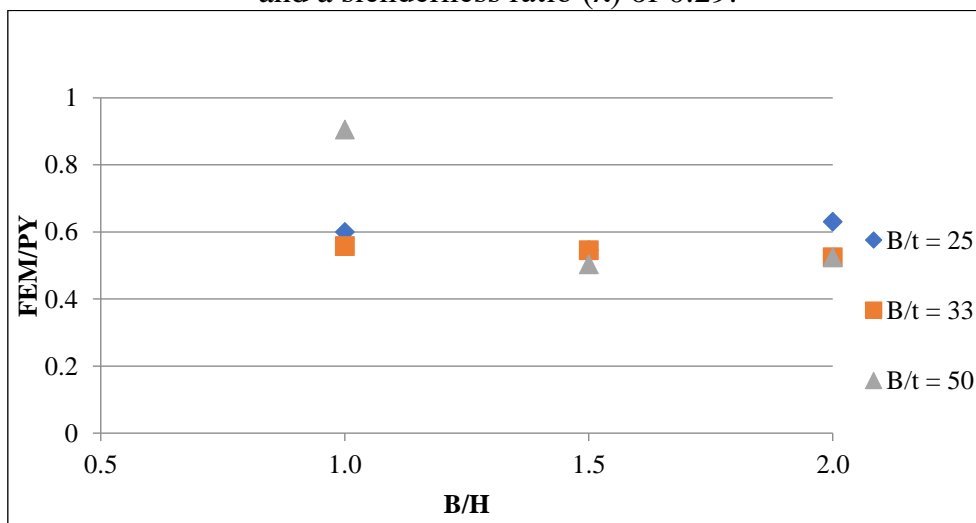Fig. 10. Relationship between B/H and FEM/P_Y for columns with different B/t values and a slenderness ratio (λ) of 0.63.
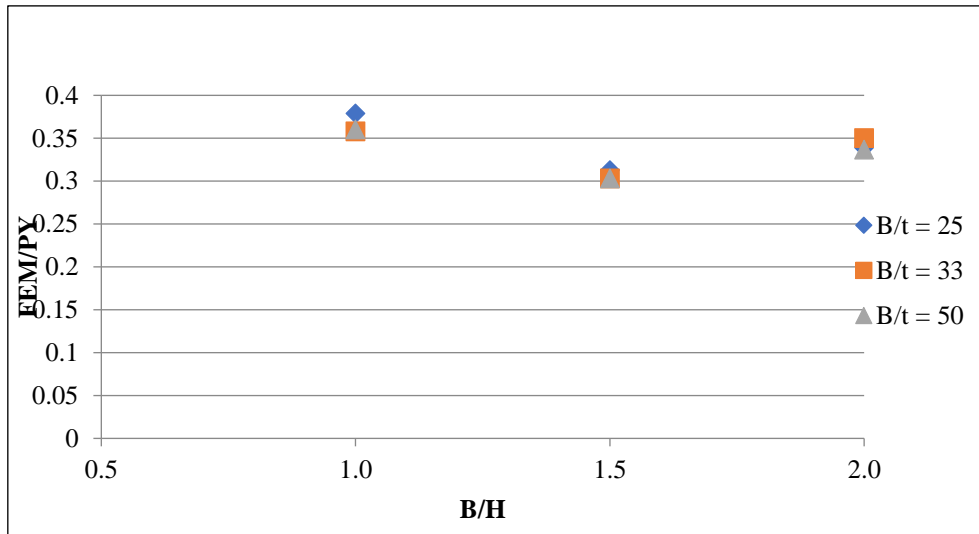
Fig. 11. Relationship between B/H and FEM/P_Y for columns with different B/t values and a slenderness ratio (λ) of 1.23.
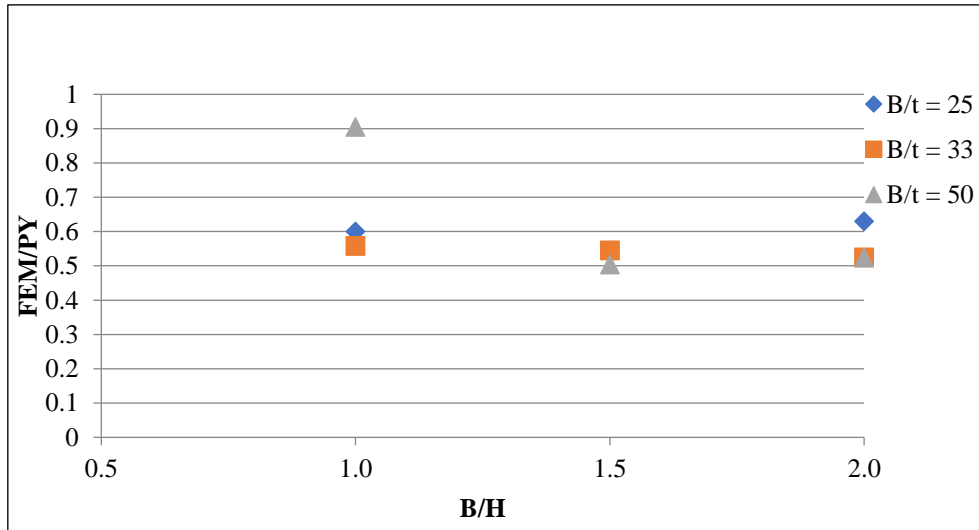

Fig. 12. Relationship between B/H and FEM/P_Y for columns with different B/t values and a slenderness ratio (λ) of 3.38.

3.1.3 Effect of global non-dimensional slenderness

It is well established that increasing non-dimensional slenderness decreases FEM/P_Y, but the results vary according to parameters such as B/t and B/H. For instance, columns with $B/H = 1$ and $B/t = 25$ exhibit a decrease of up to 62% in FEM/P_Y for $\lambda <$ 1.23 and this decrease is up to 100% for higher λ. Similarly, the decrease in columns with $B/t = 33$ reaches 64% for $\lambda < 1.23$ and is up to 93% for higher λ. For columns with

B/t = 50, the decrease is up to 63% and increases to 89% for higher λ, as shown in Fig. 13.

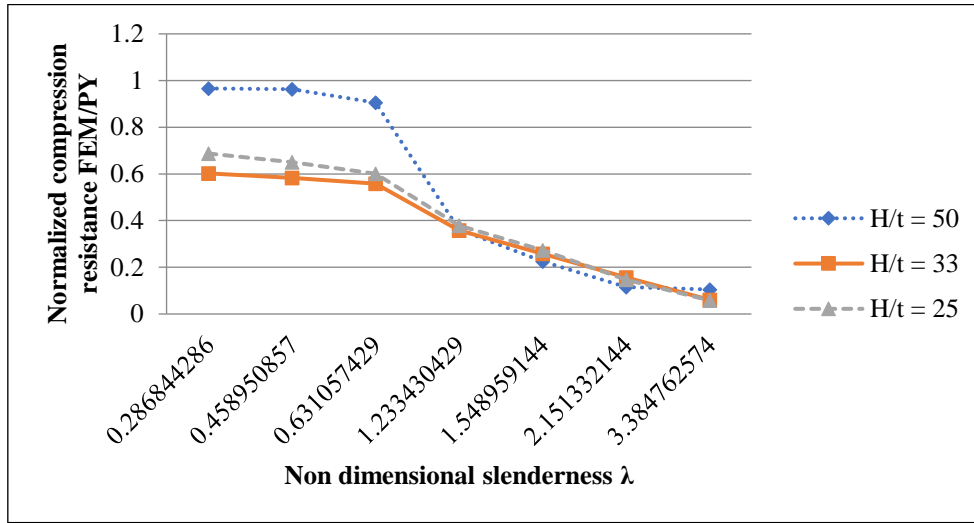Fig. 13. Relationship between global non-dimensional slenderness (λ) and FEM/P_Y for columns with *B/H* = 1 and different *B/t* values.

Columns with *B/H* = 1.5, as shown in Fig. 14, exhibit an inversely proportional relationship between λ and FEM/P_Y. When *B/t* = 25, changing λ from 0.63 to 1.23 decreases FEM/P_Y by up to 47% and by up to 93% for higher λ. Meanwhile, columns with *B/t* = 33 exhibit a decrease in FEM/P_Y by up to 68% for lower λ. Notice that changing λ from 1.23 to 3.38 decreases FEM/P_Y by 94%. Columns with *B/t* = 50 exhibit a decrease by up to 69% for λ < 1.23, and this decrease is up to 94% for higher λ.
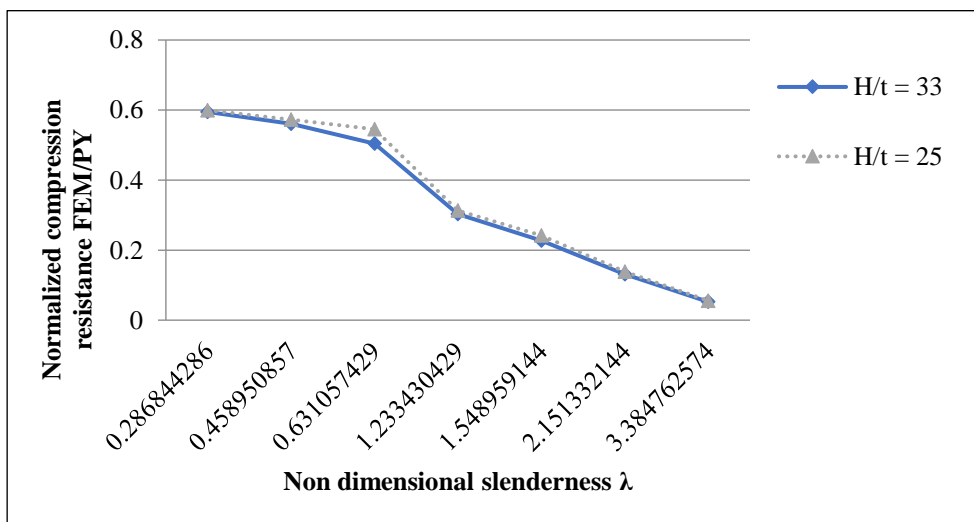

Fig. 14. Relationship between global non-dimensional slenderness (λ) and FEM/P_Y for columns with *B/H* = 1.5 and different *B/t* values

For columns with $B/H = 2$ and $B/t = 25$, as shown in Fig. 15, changing λ from 0.63 to 1.23 causes a decrease in FEM/P_Y by up to 54% and by up to 95% for higher λ. Meanwhile, columns with $B/t = 33$ exhibit a decrease in FEM/P_Y by up to 71% for lower λ. Notice that changing λ from 1.23 to 3.38 decreases FEM/P_Y by 96%. Columns with $B/t = 50$ exhibit a decrease by up to 66% for $\lambda < 1.23$, and this decrease is up to 93% for higher λ.
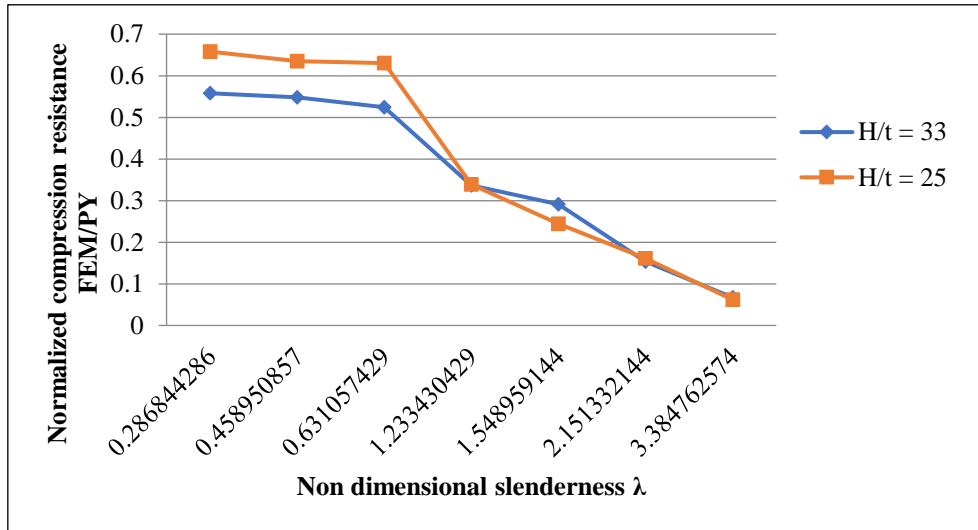

Fig. 15. Relationship between global non-dimensional slenderness (λ) and FEM/P_Y for columns with $B/H = 2$ and different B/t values.

3.2 Comparison between EURO and ECP Design Equations

It is worth mentioning that there are no design equations specifically for SEHS columns; the only available equations are for double symmetric sections. A comparison was therefore conducted among the Eurocode (EURO/P_Y), Egyptian code (ECP/P_Y), and FEM/P_Y results, as listed in Table 2. Buckling curves are plotted in Figs. 16-18, showing the relationships among λ, FEM/P_Y, EURO/P_Y, and ECP/P_Y for different columns.

For columns with $B/H = 1$ with different B/t values, the results are shown in Figs. 16-18. For columns with $B/t = 50$, good agreement in results is observed with the maximum difference in results being up to 12% in ECP and 14% in EURO. For all other columns with $B/t = 33$ and 25, good agreement in results is noticed in ECP for $\lambda \leq 0.63$, but a huge difference in results by up to 54% occurs for $\lambda > 0.63$, which is obvious in

Figs. 16 and 17. Good agreement in results is obvious from the comparison with EURO, where the greatest variation is by up 14%.

For columns with $B/H = 1.5$ corresponding to different B/t values, the results are shown in Figs. 19-21. All columns exhibit good agreement in results in ECP for $\lambda \leq 0.63$, whereas the variation in results reaches 50% for higher λ. In contrast, EURO exhibits good agreement by up to 14%.

Columns with $B/H = 2$ with $B/t = 50$ exhibit huge variations by up to a factor of 2 in ECP. However, for $B/t = 33$ and 25, the behaviour is like that of columns with $B/H = 1$ and 1.5. For EURO, good agreement in results is noticed for all columns except for columns with $B/t = 25$ for $\lambda > 0.63$, as shown in Figs. 22–24. Code equations are conservative because they neglect the role of the curved part in postcritical strength.
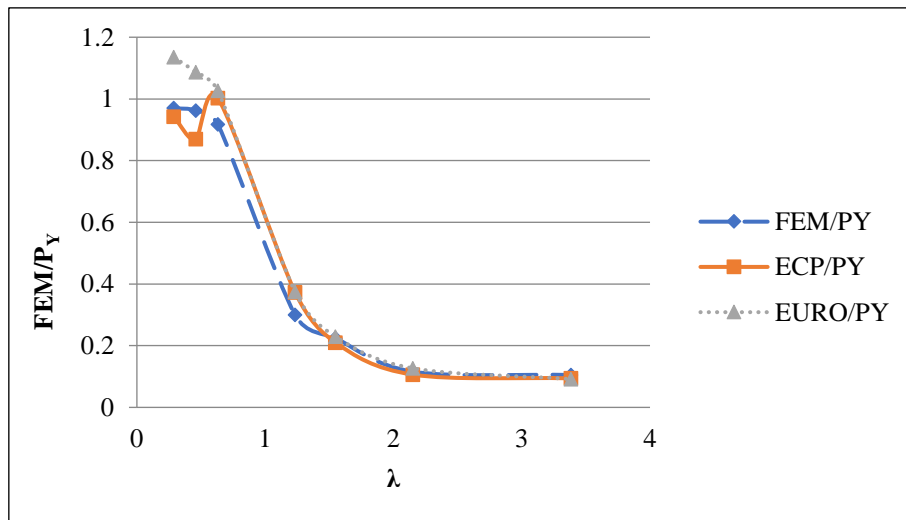

Fig. 16. Relationship between global non-dimensional slenderness (λ) and FEM/P_Y, ECP/P_Y, and EURO/P_Y for columns with $B/H = 1$ and $B/t = 50$.
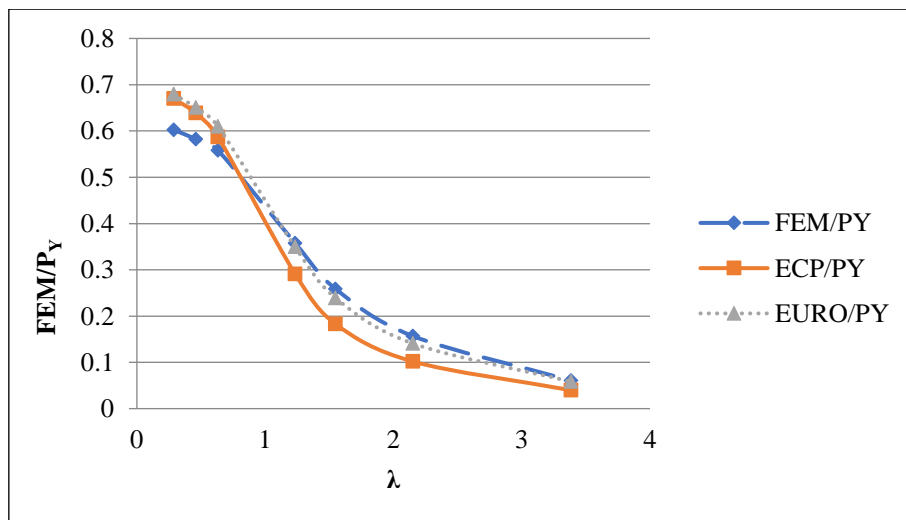

Fig. 17. Relationship between global non-dimensional slenderness (λ) and FEM/P_Y, ECP/P_Y, and EURO/P_Y for columns with $B/H = 1$ and $B/t = 33$.
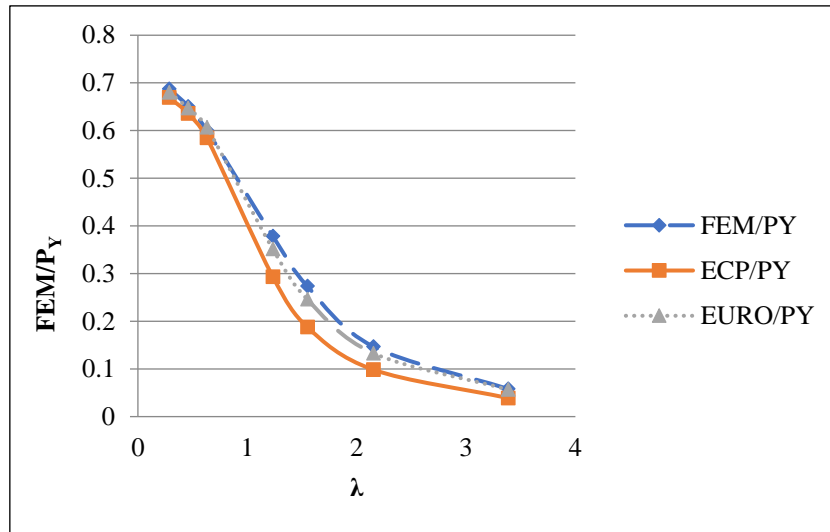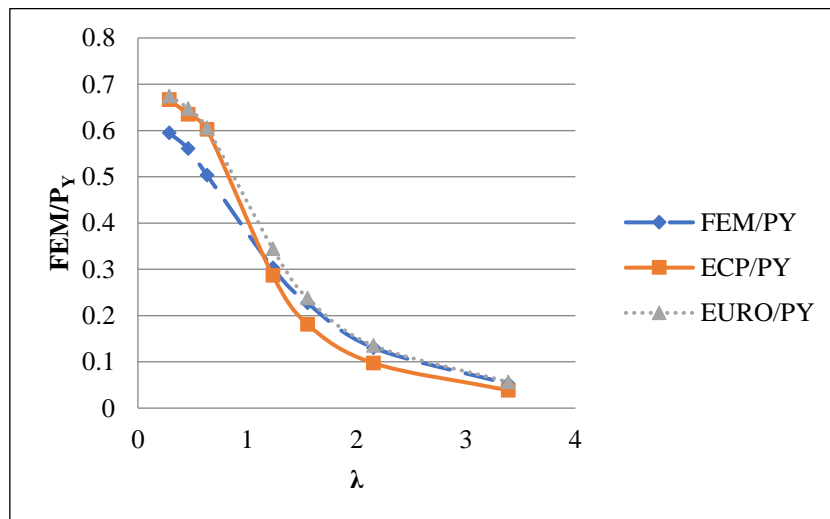
Fig. 18. Relationship between global non-dimensional slenderness (λ) and FEM/P_Y, ECP/P_Y, and EURO/P_Y for columns with $B/H = 1$ and $B/t = 25$.

Fig. 19. Relationship between global non-dimensional slenderness (λ) and FEM/P_Y, ECP/P_Y, and EURO/P_Y for columns with $B/H = 1.5$ and $B/t = 50$.

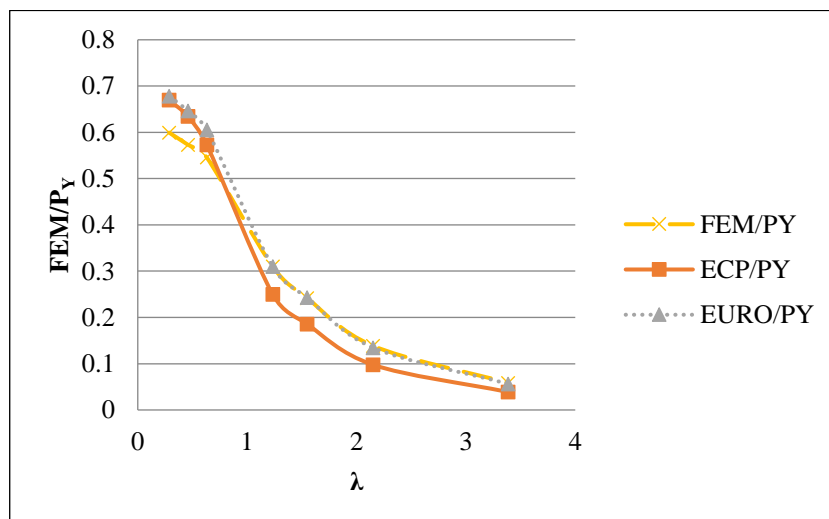Fig. 20. Relationship between global non-dimensional slenderness (λ) and FEM/P_Y, ECP/P_Y, and EURO/P_Y for columns with $B/H = 1.5$ and $B/t = 33$.

Fig. 21. Relationship between global non-dimensional slenderness (λ) and FEM/P_Y, ECP/P_Y, and EURO/P_Y for columns with $B/H = 1.5$ and $B/t = 25$.

Fig. 22. Relationship between global non-dimensional slenderness (λ) and FEM/P_Y, ECP/P_Y, and EURO/P_Y for columns with $B/H = 2$ and $B/t = 50$.

Fig. 23. Relationship between global non-dimensional slenderness (λ) and FEM/P_Y, ECP/P_Y, and EURO/P_Y for columns with $B/H = 2$ and $B/t = 33$.
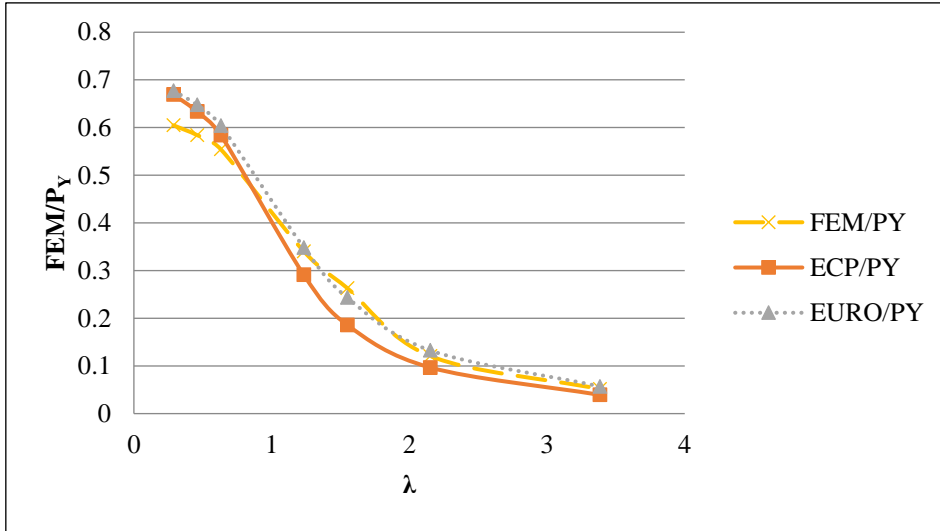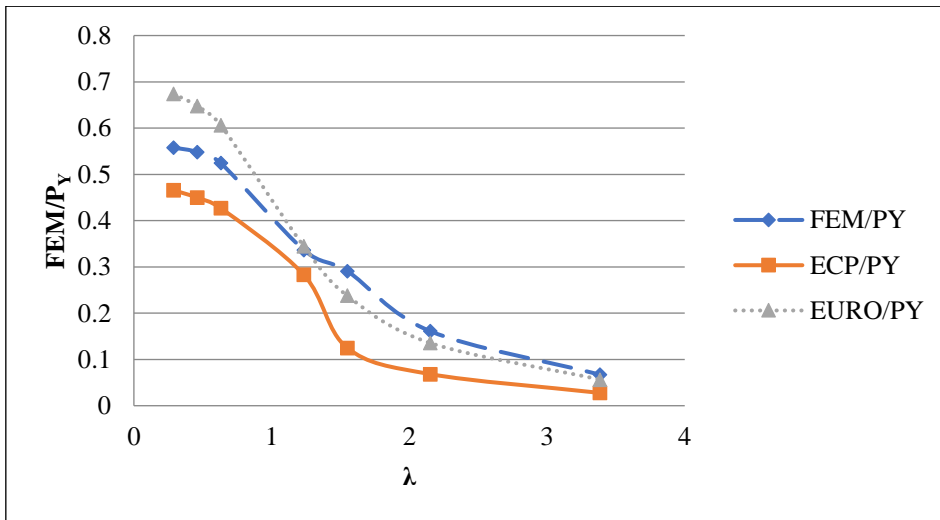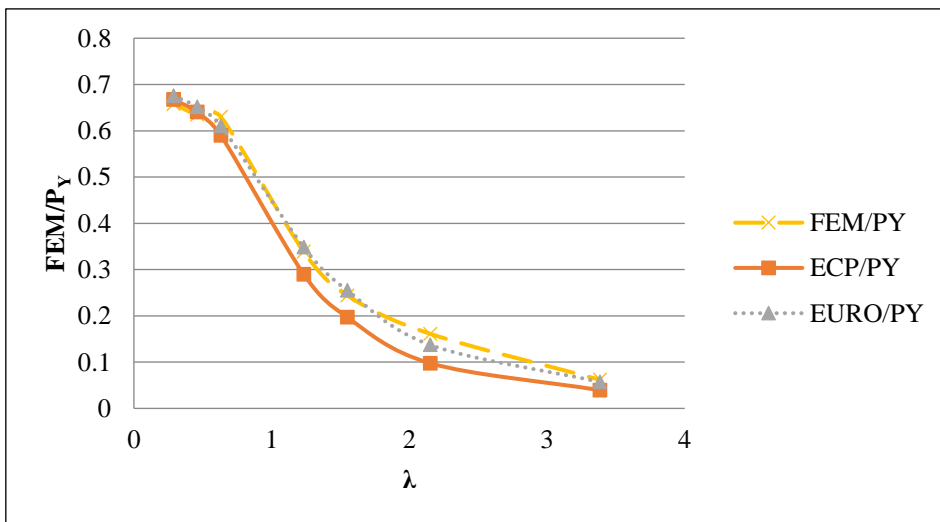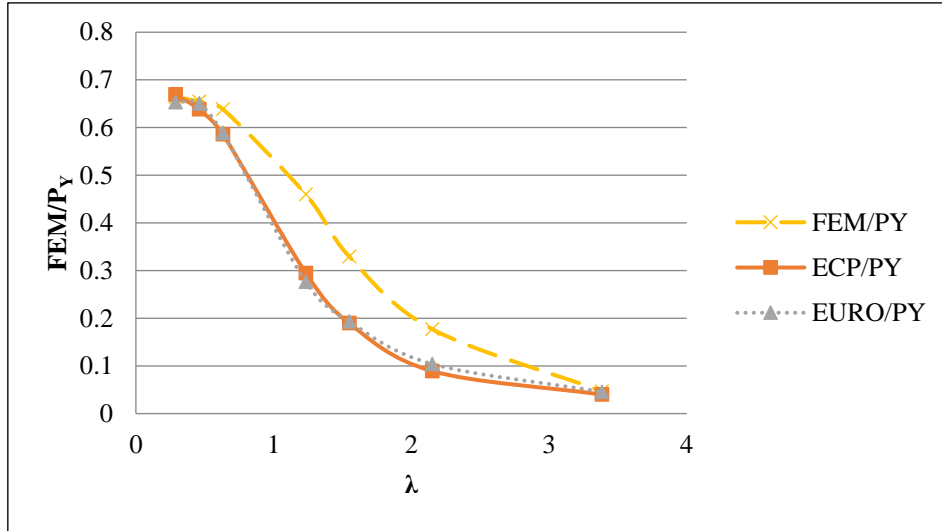
Fig. 24. Relationship between global non-dimensional slenderness (λ) and FEM/P_Y, ECP/P_Y, and EURO/P_Y for columns with $B/H = 2$ and $B/t = 25$.

3.3 Modified EURO and ECP Design Equations

In this section, regression is used to adjust the EURO equations to achieve reasonable results (Mod. EURO) for $B/H = 2$ with $B/t = 25$ and $λ > 0.63$:

$$Mod.\ EURO/P_Y = EURO/P_Y×1.75659451036312 − 0.0170327124320087. \quad (2)$$

In addition, the modified Egyptian code equations (Mod. ECP) were prepared for $B/H = 2$ and $λ > 0.63$; these results are shown in Figs. 25–27. The maximum difference in results is up to 15% according to
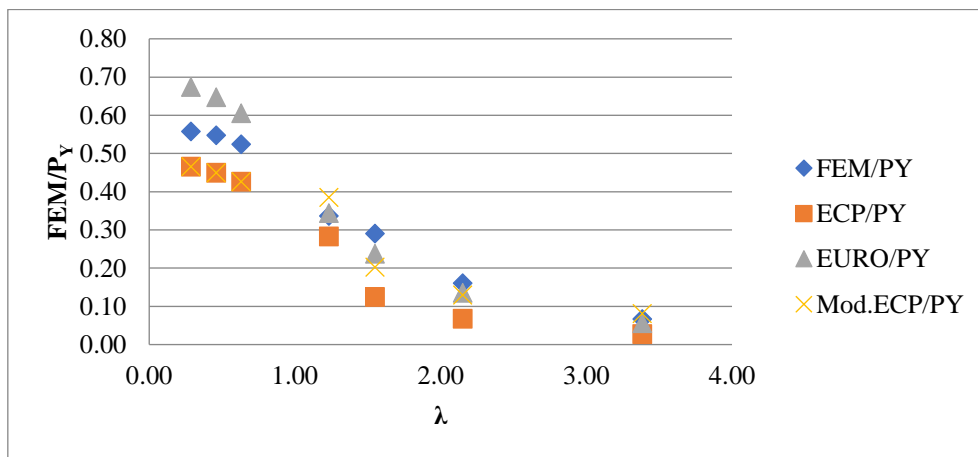
$$Mod.\ ECP/P_Y = ECP/P_Y×1.214665 + 0.045361. \quad (3)$$

Fig. 25. Relationship between global non-dimensional slenderness (λ) and FEM/P_Y, ECP/P_Y, EURO/P_Y, and Mod. ECP/P_Y for columns with $B/H = 2$ and $B/t = 50$.
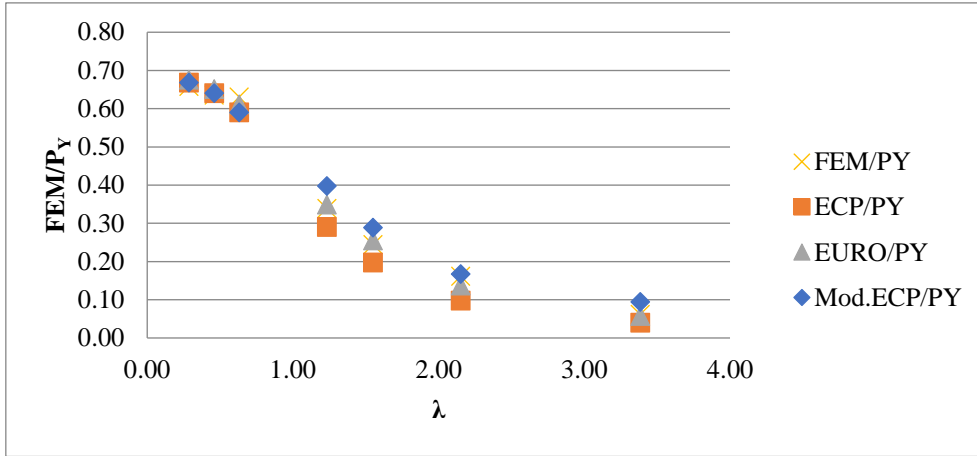
Fig. 26. Relationship between global non-dimensional slenderness (λ) and FEM/P_Y, ECP/P_Y, EURO/P_Y, and Mod. ECP/P_Y for columns with $B/H = 2$ and $B/t = 33$.
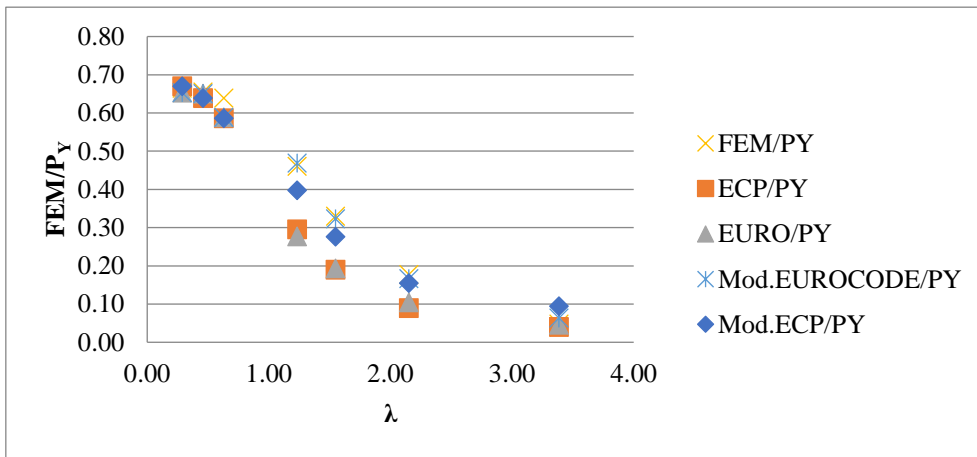

Fig. 27. Relationship between global non-dimensional slenderness (λ) and FEM/P_Y, ECP/P_Y, EURO/P_Y, Mod. EURO/P_Y, and Mod. ECP/P_Y for columns with $B/H = 2$ and $B/t = 25$.

4. CONCLUSIONS

This study focuses on the behaviour of SEHS columns under axial force. The results show that, when sections with a local slenderness ratio of 50 (slender) are compared to those with local slenderness ratio of 33 (non-compact), an increase in the ultimate load to yield ratio by up to 30% for global non-dimensional slenderness of <1.23 is noticed when the aspect ratio is 1. Meanwhile, for the same sections, a decrease in the ultimate load to yield ratio by up to 92% is noticed for global non-dimensional slenderness of >1.23. When the local slenderness ratio is changed from 25 or 33 to 50 for columns with aspect ratios of 1.5 and 2, FEM/P_Y is reduced along with an increase in the global non-dimensional slenderness by up to 100%. Finite element results show

that changing the aspect ratio from 1 to 1.5 or 2 in all columns decreases FEM/P_Y by up to 40% for global non-dimensional slenderness of <1.23 and by up to 94% for higher values. EURO gives good agreement with these results for all columns except compact columns with an aspect ratio of 2. In contrast, the Egyptian code gives accurate results for slender sections, but it is conservative in compact and non-compact ones with higher global non-dimensional slenderness. Modified design equations for SEHS columns are prepared based on the analytical results where good agreement in results is observed.

DECLARATION OF CONFLICTS OF INTEREST

The authors have declared no conflicts of interest.

REFERENCES

1. Chan, T. M., and Gardner, L., "Flexural Buckling of Elliptical Hollow Section Columns", Journal of Structural Engineering-ASCE, Vol. 135, No. 5, pp. 546-557, 2009.
2. Ruiz-Teran, A. M., and Gardner, L., "Elastic Buckling of Elliptical Tubes", Thin Walled Structures, Vol. 46, pp. 1304-1318, 2008.
3. Bradford, M. A., and Roufegarinejad A., "Elastic Local Buckling of Thin Walled Elliptical Tubes Containing Elastic Infill Material", Interaction and Multiscale Mechanics, Vol. 1, No.1, pp. 143-156, 2008.
4. Nowzartash, F., "Plastic Interaction Relations for Elliptical and Semi-Elliptical Hollow Sections", Ph. D. Thesis, Civil Engineering Department, Faculty of Engineering University of Ottawa, 2011
5. Quach, W., and Young, B., "Rolled Elliptical Hollow Sections", Advances in Structural Engineering, Vol. 18, No. 7, pp. 1101-1114, 2015.
6. Fang, C., Zhou, F., and Wu, W., "Performance of Elliptical Hollow Sections under Combined Compression and Cyclic Bending", Journal of Structural Engineering, Vol. 144, No. 8, 2018.
7. Kotab, M. A., Ramadan, H. M., and Mourad, S. A., "Behavior of Rectangular Concrete Filled Steel Tubes Subjected to torsion", Journal of Engineering and Applied Science, Vol. 62, No. 1, pp. 45-60, 2015.
8. Silvestre, N., Pires, T., and Duarte, A. P. C., "Numerical Analysis of Semi-Elliptical Hollow Section Columns", Structures and Buildings, Proceedings of the Institution of Civil Engineers, Vol. 166, No. 8, 2015.
9. EN 1993-1-3, "Eurocode 3: Design of Steel Structures, Part 1-3: General rules, Supplementary rules for steel, European Committee for Standardization CEN, Europe 2006.
10. ECP 205 (LRFD), "Egyptian Code of Practice for Steel Construction and Bridges", Housing and Building Research Center, Giza, Egypt, 2007.

LIST OF SYMBOLS

B, *H*, and *t*	Flat part width, curved part width, and thickness of the semi-elliptical section, respectively
λ	Global non-dimensional slenderness
E and F_y	Modulus of elasticity and the yield stress of steel
K	Buckling length factor
L	Unsupported length
r	Radius of gyration about minor axis

<div dir="rtl">

قطاعات الأعمدة المفرغة النصف بيضاوية تحت تأثير الأحمال المحورية

يتناول البحث ســلوك الأعمدة ذات القطاعات البيضــاوية المفرغة تحت تأثير الحمل المحورى.تم اعداد دراســة بارامترية باســتخدام نموذج تحليل عددى بعد مقارنة نتائجه مع الابحاث الســابقة. الدراســة أخذت فى الاعتبار عدد من العوامل المؤثرة مثل نحافة القطاع والنسبة بين الأبعاد. لابد من الاشارة أنه لا توجد معادلات تصــميمية تخص هذا القطاع تحديدا وبناءا عليه تم اســتخدام نتائج نموذج التحليل العددى فى تعديل المعادلات الموجودة فى كل من الكود المصري والكود الأوروبي.

</div>